









Synthesis and characterization of carbon nanomaterials obtained using electric discharge

M.K. Kazankapova^{1,2,3} , B.T. Yermagambet^{1,2,3} , B.K. Kasenov⁴ ,
Zh.M. Kassenova^{1,2,3} , A.B. Malgazhdarova^{1,2*} , G.K. Mendaliyev^{1,2} ,
A.S. Akshekina¹  and U.M. Kozhamuratova^{1,2} 

¹«Institute of Coal Chemistry and Technology» LLP, Astana, Kazakhstan

²L.N. Gumilyov Eurasian National University, Astana, Kazakhstan

³Kazakh university of technology and business named after K. Kulazhanov, Astana, Kazakhstan

⁴«Chemical and Metallurgical Institute named after Zh. Abisheva», Karagandy, Kazakhstan

*e-mail: coaltech@bk.ru

(Received March 3, 2025; received in revised form May 13, 2025; accepted May 23, 2025)

In recent years, carbon nanomaterials have been studied for their applications in important areas of engineering and technology due to their unique physical, chemical, and biological properties. The high demand for developing carbon nanomaterials through environmentally friendly and low-cost synthesis strategies has resulted in significant efforts being undertaken worldwide. This study presents the synthesis and characterization of carbon nanomaterials (CNMs) using the electric arc discharge method under conditions of 75 V and 100 A. A copper substrate was employed to promote material deposition. Structural and morphological properties were examined using SEM and Raman spectroscopy. The results revealed the formation of multilayer carbon nanostructures with a high degree of graphitization (up to 88.98%) and particle sizes ranging from 38 to 53.5 nm. Electrophysical measurements demonstrated high dielectric constants and semiconducting behavior over the temperature range of 293–483 K, indicating the material's potential for electronic applications. The synthesis method offers a scalable, cost-effective, and environmentally friendly approach to producing high-quality carbon nanomaterials.

Key words: carbon nanotubes (CNTs), graphitization, temperature dependence, nanostructured materials, graphitic structures.

PACS number(s): 82.33; Pt 82.80.– d.

1 Introduction

The use of carbon nanomaterials, including CNTs and fullerenes, is currently of great importance in various modern areas of nanotechnology, new technological processes, and the creation of new high-performance and high-quality materials in biological engineering [1].

Carbon materials are materials with high strength, thermal and electrical conductivity, and chemical stability. They are widely used in many industries. In recent years, novel carbon nanostructures and so-called carbon-carbon nanocomposites have been theoretically predicted and successfully synthesized. These materials exhibit distinct atomic structures, well-defined dimensions, and diverse morphologies, leading to a broad spectrum of unique physical and chemical

properties [2,3]. The electro-discharge technique is extensively utilized for synthesizing superior-quality carbon nanotubes (CNTs) as it operates at exceptionally elevated temperatures [4]. An overview of various classes of carbon nanomaterials synthesized from coal is presented in Figure 1.

The chemical bonding in carbon nanotubes (CNTs) is entirely composed of sp²-hybridized bonds, which are significantly stronger than the sp³ bonds found in alkanes, thereby imparting exceptional mechanical strength to CNTs [5]. Notably, CNTs exhibit an extraordinarily high length-to-diameter ratio, reaching up to 132,000,000:1, which surpasses that of any other known material [6].

Thanks to their distinctive hexagonal carbon framework, CNTs exhibit exceptional electrical, mechanical, and thermal characteristics, rendering

them highly adaptable for numerous applications in diverse scientific and industrial domains [7,8]. As members of the fullerene family, CNTs derive their name from their elongated, hollow, hexagonal cylindrical structure, characterized by single-atom-thick walls composed of carbon sheets known as graphene. These graphene layers are rolled up at specific chiral angles, which ultimately determine the electronic and mechanical properties of the resulting CNTs. The ends of CNTs are typically capped with a fullerene-like molecular structure [9].

Structurally, CNTs are divided into two primary categories: single-walled carbon nanotubes (SW-CNTs) and multi-walled carbon nanotubes (MW-CNTs). Each of these structures arranges itself into bundles, held together by van der Waals forces, forming rope-like assemblies with enhanced mechanical stability [10].

The primary application areas of carbon nanotubes (CNTs) include electronics, medicine, chemistry, pharmaceuticals, and biology. However, the selection of an appropriate CNT synthesis method is a critical factor when considering their potential for various applications. The assessment of different synthesis techniques is typically based on key criteria such as cost-effectiveness, raw material conversion

efficiency, and process controllability [11].

After comparing many international and domestic literature data, the electric arc discharge method was selected as one of the most effective methods for producing carbon nanomaterials. This method is based on connecting two graphite electrodes with a high current in an inert gas atmosphere, creating a stable arc discharge between them, which ensures the evaporation of graphite at high temperatures and the formation of carbon nanostructures. These methods ensure scalable and effective CNT production while allowing precise control over their structural features [12].

Currently, there are several common methods for synthesizing CNTs, namely thermal plasma [13], chemical vapor deposition (CVD) [14], and arc discharge [15] methods. Several researchers, based on their research results [16], first developed a thermal plasma method for obtaining multi-walled CNTs from carbon, and secondly, a method based on the thermal decomposition of carbon-containing gases (chemical vapor deposition) accompanied by gas-phase chemical deposition of crystalline nanocarbons on metal. Accordingly, the most effective of these methods was found to be the electric arc discharge method.

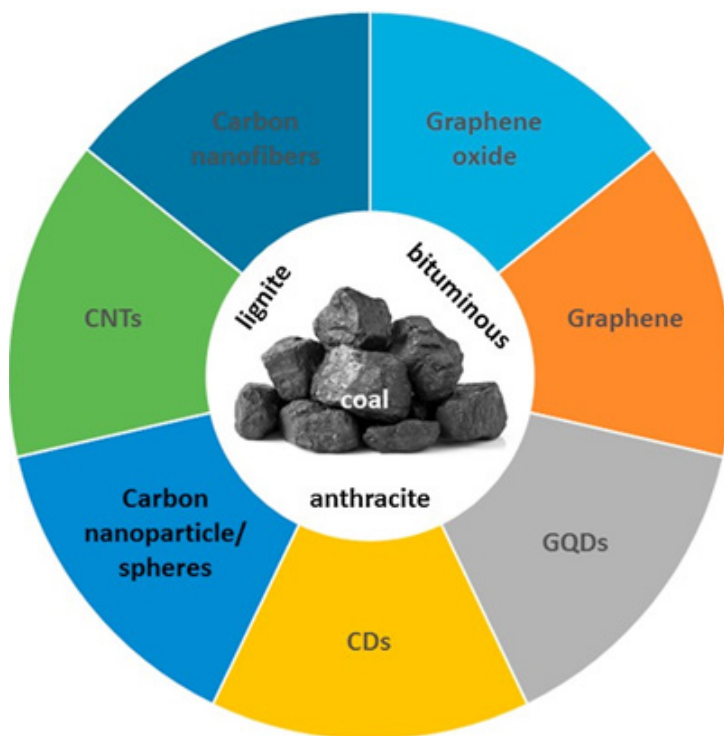


Figure 1 – Types of carbon nanomaterials obtained from different types of coal.

One of the first to synthesize carbon nanomaterials using the electric arc discharge method was the Japanese scientist Sumio Iijima [17]. He studied and characterized the structure of the an-

ode formed by generating an electric arc discharge using a microscope. The electric arc discharge is caused by high current and very high temperature (fig. 2).

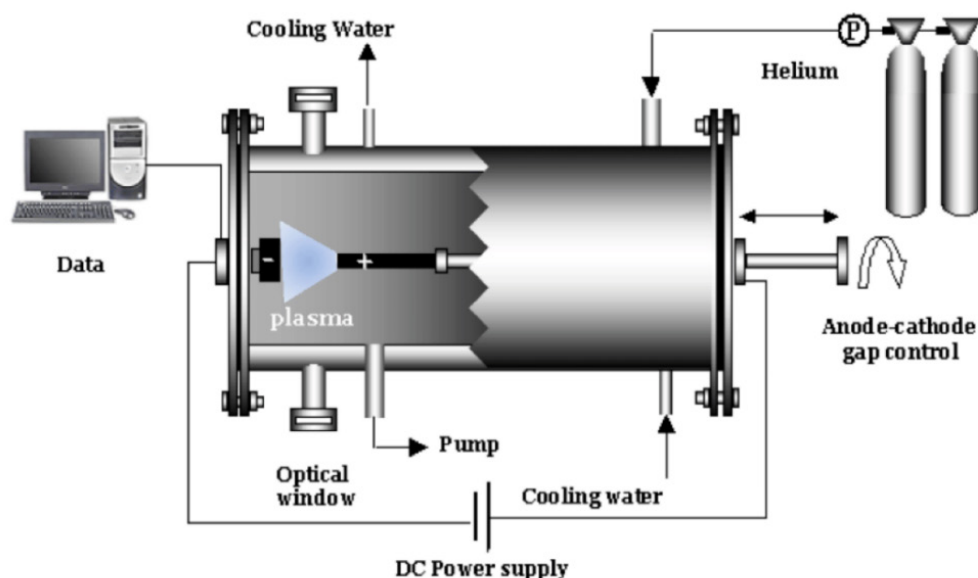


Figure 2 – Production of carbon nanotubes using the electric arc discharge method.

Summarizing the reviewed literature, the electric arc discharge method can be considered as the most optimal method for synthesizing carbon nanotubes, which uses plasma-chemical and thermodynamic processes to generate carbon nanostructures from carbon-based plasma. This method is widely recognized for its cost efficiency, high raw material conversion rate, and controllability of the synthesis process, making it highly suitable for large-scale CNT production [19].

During the electric discharge process, a high-current arc is established between graphite electrodes in an atmosphere of inert gas, resulting in the evaporation of carbon, which subsequently condenses into nanotubular structures. The controlled parameters of this method, including arc current, voltage, gas composition, and pressure, enable precise tailoring of CNT properties, such as diameter, length, and defect density. Due to these advantages, the electric discharge method remains a promising approach for synthesizing high-purity CNTs with well-defined structural characteristics, facilitating their integration into applications in electronics, medicine, chemistry, pharmaceuticals, and biotechnology [20].

The electric arc discharge method remains one of the most efficient and scalable techniques for the

synthesis of various carbon nanomaterials (CNMs), including fullerenes, carbon nanotubes (CNTs), graphene, carbon nanohorns, and core-shell nanoparticles. In recent years, significant progress has been made in understanding the mechanisms governing the formation and structural evolution of these materials under arc plasma conditions.

Roslan et al. (2018) studied the transformation of fullerenes into multi-walled carbon nanotubes (MW-CNTs) using arc discharge plasma, revealing insights into the gradual structural reorganization of carbon species during the synthesis process [21]. Complementarily, Raniszewski (2018) demonstrated that the application of an external electromagnetic field during arc discharge leads to a noticeable improvement in CNT yield and crystallinity, opening new avenues for controlled synthesis [22].

Further development in the control of product morphology was achieved by Zhang et al. (2019), who showed that varying the buffer gas type and pressure enables selective synthesis of different nanocarbon structures, including fullerenes, graphene, and nanohorns, within the same arc reactor [23]. Another noteworthy study by Zaikovskii et al. (2019) reported the formation of tin-carbon core-shell nanoparticles during arc discharge in helium, providing insight into

metal-carbon interaction and encapsulation mechanisms in plasma conditions [24].

In addition to arc systems operating in noble gases, the synthesis of carbon nanosheets has been successfully conducted in gliding arc reactors. Ma *et al.* (2021) compared chemical vapor dissociation of toluene with graphite exfoliation, demonstrating that process parameters significantly affect the morphology and surface structure of the resulting nanosheets [25].

A deeper understanding of nanoparticle formation dynamics in carbon arc plasma was provided by Yatom *et al.* (2018), who combined experimental diagnostics with numerical modeling. Their findings revealed that carbon nanoparticles predominantly nucleate in the peripheral regions of the arc, where temperature and carbon vapor gradients are optimal for nucleation and growth [26].

Arc discharge techniques have also been adapted for the synthesis of carbon nanomaterials from coal-derived precursors. A 2021 study reported the fabrication of graphene-containing nanostructures using electric arc treatment of coke derived from Shubarkol brown coal. These materials exhibited promising structural characteristics suitable for applications in energy storage and catalysis [27].

Overall, the arc discharge technique continues to be a powerful and versatile tool for producing high-quality carbon nanomaterials. The ability to control synthesis parameters—such as gas type, pressure, electrode composition, and external fields—provides wide tunability in nanomaterial structure and functionality. Future work will likely focus on process scaling, hybrid nanomaterials, and integration into device applications.

Carbon nanomaterials, particularly carbon nanotubes (CNTs), have been widely investigated due to their exceptional mechanical, thermal, and electrical properties. Numerous synthesis techniques have been developed, with the electric arc discharge method recognized for its high purity and crystallinity of produced CNTs. However, despite extensive research, limited attention has been paid to the use of copper substrates in arc discharge synthesis, and the resulting structural, morphological, and electrophysical properties of the synthesized CNMs remain insufficiently explored. In this study, we introduce a novel approach using a copper substrate in the electric arc discharge method (100 A, 75 V) to synthesize carbon nanomaterials. We characterize the resulting nanostructures using SEM and Raman spectroscopy and evaluate their electrophysical properties over a wide temperature range. This work provides new in-

sights into scalable production of CNMs with high dielectric constants and tunable electrical behavior, highlighting their potential for advanced electronic applications [28].

2 Materials and methods

The electric arc discharge method (100 A, 75 V) was employed to obtain nanomaterials. Pyrolysis gas acted as the carbon source, while graphite was used for the electrode and a copper plate as the substrate. The synthesis of carbon nanomaterials was carried out using the electric arc discharge method under the following conditions: a DC power source provided a stable discharge current of 100 A at a voltage of 75 V between two high-purity graphite electrodes. The discharge was conducted in a sealed stainless-steel chamber filled with argon gas (99.999% purity) at a pressure of 400 Torr (approximately 53 kPa). A continuous argon flow rate of 1.5 L/min was maintained throughout the process to ensure an inert atmosphere and remove reaction by-products. The inter-electrode gap was set at approximately 2 mm, and the arc discharge was sustained for 10 minutes per synthesis run. The copper substrate was positioned below the electrode assembly to collect deposited carbon material, while additional deposition occurred on the reactor wall and electrode surface. The analysis was performed using a laboratory carbonization furnace, gas chromatograph, scanning electron microscope, and Raman spectroscopy.

The chemical analysis and surface morphology of the samples were studied using energy dispersive X-ray spectroscopy on an SEM (Quanta 3D 200i) with an EDAX energy dispersive analyzer. SEM images were obtained with the Quanta 3D 200i field-emission gun (FEG) at magnifications of $\times 2000$, $\times 10000$, and $\times 50000$. A 5 nm conductive gold coating was applied to the samples using a Q150T ES sputter coater (Quorum Technologies, UK) to prevent charging effects during imaging.

The SEM system was operated under high-vacuum mode, with an accelerating voltage of 5–15 kV, depending on the sample's conductivity and required resolution. Energy-dispersive X-ray spectroscopy (EDS) was performed using an EDAX Apollo X detector integrated into the SEM system to analyze the elemental composition of the samples.

Raman spectroscopy analysis was performed using an NT-MDT NTEGRA Spectra system, which provides high spatial and spectral resolution for carbon nanomaterial characterization. A 532 nm solid-state laser was used as the excitation source, with an

output power of 5 mW to prevent sample degradation. The spectral range was set from 500 to 3500 cm^{-1} , with a spectral resolution of 1 cm^{-1} . Measurements were carried out using a 100 \times objective lens ($\text{NA} = 0.95$), providing a spatial resolution of approximately 300 nm. The system was calibrated prior to each measurement using the 520.7 cm^{-1} silicon peak as a reference. The acquisition time for each spectrum varied between 10 and 30 seconds, depending on the fluorescence level of the sample. The intensity ratios ID/IG and I2D/IG were calculated to evaluate the degree of graphitization, defect density, and multilayer nature of the synthesized carbon nanomaterials. Data processing and spectral deconvolution were conducted using Nova PX software, ensuring precise background correction and peak fitting.

Measurement of electrical properties (dielectric constant ϵ , electrical resistance R) was carried out by measuring the electrical capacitance C of samples on a serial LCR-800 device (L , C , R meter) at an operating frequency of 1, 5, 10 kHz with a base error of 0.05-0.1%.

Plane-parallel samples were pre-fabricated in the form of disks with a diameter of 10 mm and a thickness of 1-6 mm with a binder additive ($\sim 1.5\%$). The pressing process was performed under a pressure of 20 kg/cm^2 . The resulting discs were then fired in a silit furnace at 200 $^{\circ}\text{C}$ for 6 hours. Afterward, they were carefully polished on both sides.

The dielectric constant was determined from the electrical capacitance of the sample at known values of the sample thickness and the surface area of the electrodes. To obtain the relationship between electrical induction D and electric field strength E , the Sawyer-Tower circuit was used. Visual observation of D (E of the hysteresis loop) was carried out on an S1-83 oscilloscope with a voltage divider consisting of a resistance of 6 m Ω and 700 k Ω , and a reference capacitor of 0.15 μF . Generator frequency 300 Hz. In all temperature studies, samples were placed in an oven, the temperature was measured with a chromel-alumel thermocouple connected to a B2-34 voltmeter with an error of ± 0.1 mV. Temperature change rate 5 K/min. The dielectric constant at each temperature was determined by the formula:

$$\epsilon = \frac{C}{C_0} \quad (1)$$

where $C_0 = \frac{\epsilon_0 \cdot S}{d}$ is the capacitance of the capacitor without the test substance (air).

The band gap (ΔE) of the test substance was calculated using the following formula:

$$\Delta E = \frac{2kT_1T_2}{0.43(T_2 - T_1)} \lg \frac{R_1}{R_2}, \quad (2)$$

The calculation of the band gap (ΔE) was performed using the formula, where k denotes the Boltzmann constant ($8.6173303 \times 10^{-5} \text{ eV} \cdot \text{K}^{-1}$), R_1 is the resistance at temperature T_1 , and R_2 is the resistance at temperature T_2 .

To confirm the reliability of the results, the dielectric constant of the standard substance barium titanate (BaTiO_3) was measured at 1 kHz, 5 kHz, and 10 kHz frequencies.

To ensure clarity in sample identification throughout the study, the synthesized carbon nanomaterials were categorized based on their collection location and assigned the following labels: S1 refers to the sample collected from the reactor wall, S2 corresponds to the material deposited on the copper substrate, E1 designates the sample obtained from the graphite electrode under gas-phase deposition conditions, and E2 represents the electrode-derived sample formed under solid-state conditions without the involvement of gas. These designations are consistently used in the subsequent sections to distinguish between the different sample types.

3 Results

Scanning electron microscopy (SEM) analysis of nanomaterials obtained from the reactor wall indicates the formation of flakes and finely dispersed agglomerates with different particle sizes 104-116 nm. In the Raman spectra of the sample, two typical peaks are observed at 1361 cm^{-1} and 1590 cm^{-1} , corresponding to the D and G band. They are associated with the disordered structure, defects and ordered graphitic carbon structure of carbon materials. The material possesses a limited degree of graphitization ($G_f = 36.08\%$). A key indicator of carbon material quality, the ID/IG intensity ratio, was determined, while the I2D/IG value of 0.247 (notably lower than the >1.6 observed in monolayer graphene) and the IG/I2D ratio of 4.04 support the presence of a multilayer CNT structure. The ID/IG ratio of 1.05 suggests a considerable number of defects within the material. (Fig. 3,4).

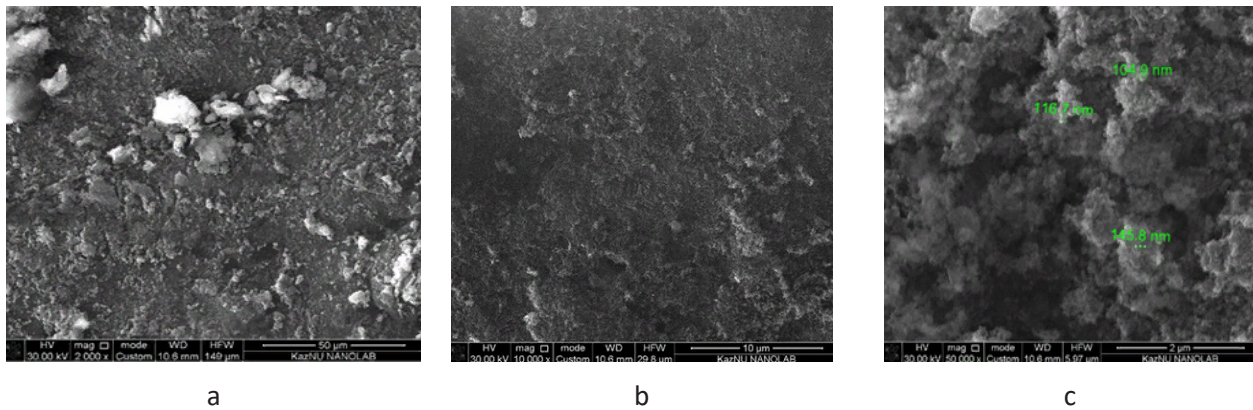
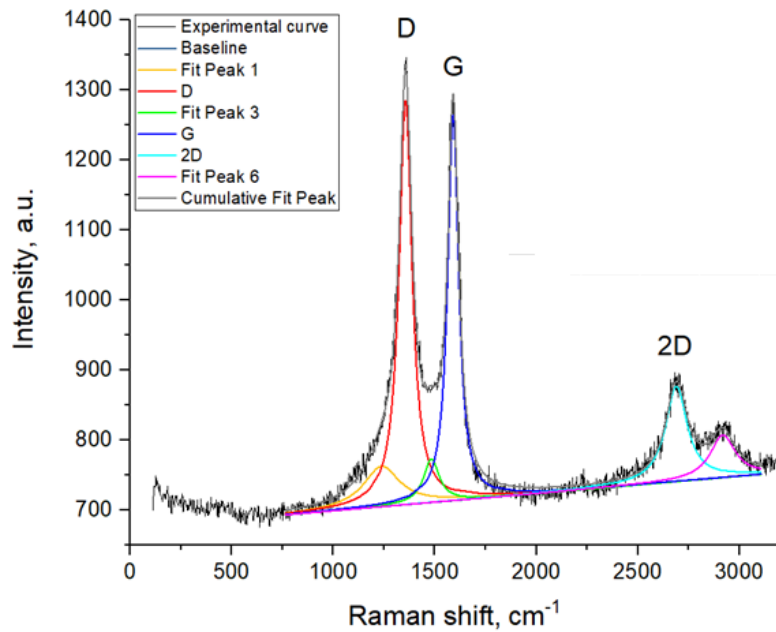


Figure 3 – SEM images of sample S1 (100 A, 75 V). a – x2000, b – x10000, c – x50000.



$$G_i = 36.08\%, I(D)/I(G) = 1.05, I(G)/I(D) = 0.95, I(G)/I(2D) = 4.04 \text{ (Lorentz)} \quad I(2D)/I(G) = 0.247$$

$$D = 1361 \text{ cm}^{-1}; G = 1590 \text{ cm}^{-1}; 2D = 2693 \text{ cm}^{-1}$$

Figure 4 – Raman spectrum of sample S1 (100 A, 75 V).

The SEM images of the sample obtained from the substrate exhibit a graphite-like signal with visible flake-shaped particles measuring between 43 nm and 51 nm. Raman spectroscopy shows characteristic peaks at D (1354; 1341 cm^{-1}) and G (1579; 1588 cm^{-1}). The ID/IG intensity ratio, commonly used to assess carbon material quality, suggests a

graphitization degree of 38.08%. The measured I2D/IG values (0.217 and 0.11) are much lower than the typical value for single-layer graphene (>1.6), while IG/I2D ratios (4.6 and 8.99) indicate a multilayer structure. The ID/IG ratios (0.64 and 1.025) reveal a significant number of defects in the material (Fig. 5,6).

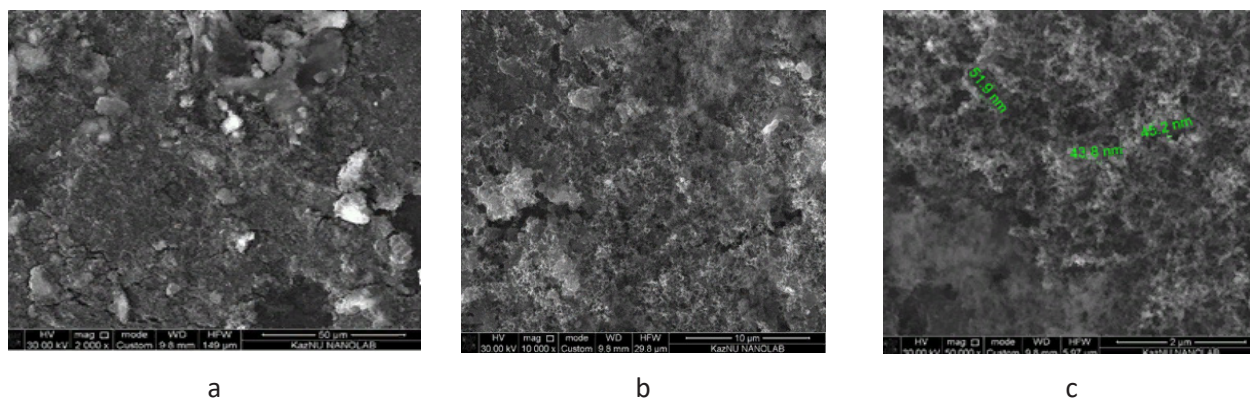
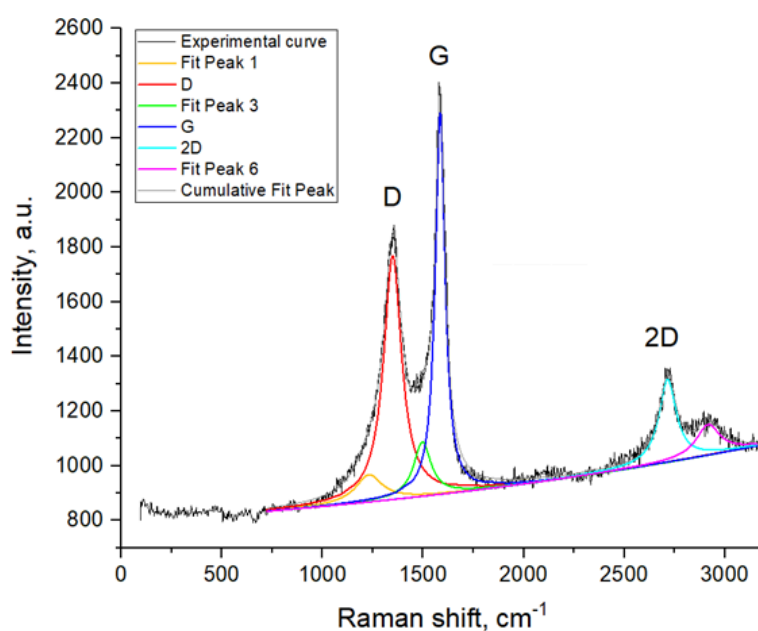


Figure 5 – SEM images of sample S2 (100 A, 75 V). a – x2000, b – x10000, c – x50000.



$G_f=38.08\%$, $I(D)/I(G)=0.64$, $I(G)/I(D)=1.56$, $I(G)/I(2D)=4.6$ (Lorentz) $I(2D)/I(G)=0.217$
 $D = 1354 \text{ cm}^{-1}$; $G = 1579 \text{ cm}^{-1}$; $2D = 2716 \text{ cm}^{-1}$

Figure 6 – Raman spectrum of sample S2 (100 A, 75 V).

Nanomaterials obtained from the electrode, as observed in SEM images, consist of flakes and small spherical agglomerates with particle sizes of 38–53.5 nm. Raman analysis confirms the formation of few-layer graphene or CNM, with characteristic peaks at 1360 cm^{-1} (D band) and 1575 cm^{-1} (G band). The graphitization degree was determined to be 88.98%,

and the ID/IG intensity ratio, which assesses carbon material quality, was examined. The I2D/IG ratio (0.39) is significantly lower than that of monolayer graphene (>1.6), while the IG/I2D ratio (2.54) supports the presence of a low-layered carbon nanomaterial. The ID/IG ratio of 0.86 suggests minimal structural defects in the analyzed sample (fig. 7,8).

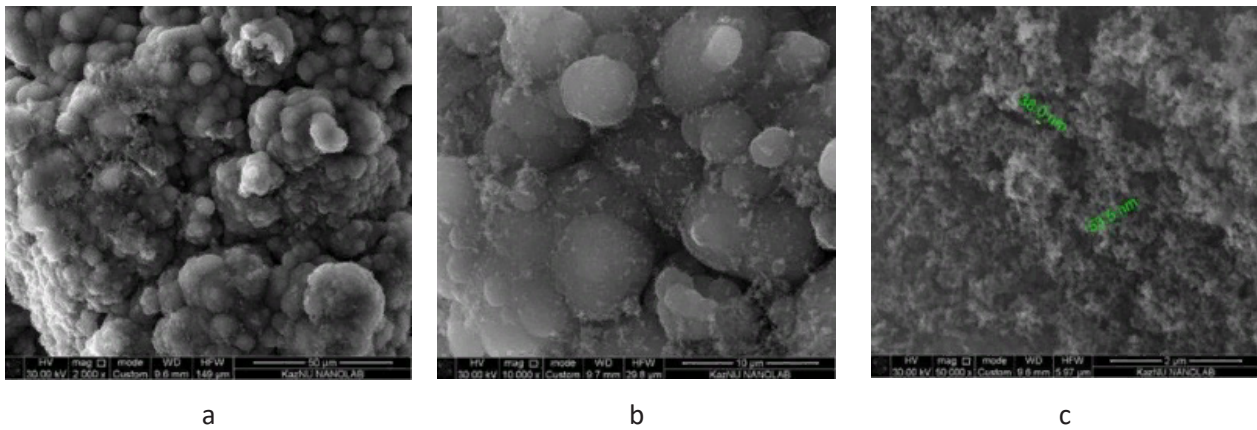
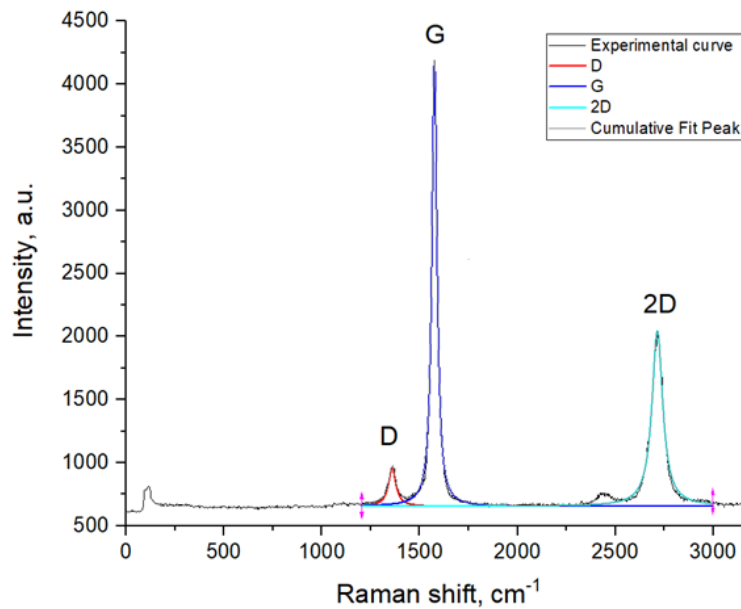


Figure 7 – SEM images of sample E1 (100 A, 75 V). a – x2000, b – x10000, c – x50000.



$$G_f = 88.98\%, I(D)/I(G) = 0.085, I(G)/I(D) = 11.72, I(G)/I(2D) = 2.54 \text{ (Lorentz)} \quad I(2D)/I(G) = 0.39$$

$$D = 1360 \text{ cm}^{-1}; G = 1575 \text{ cm}^{-1}; 2D = 2716 \text{ cm}^{-1}$$

Figure 8 – Raman spectrum of sample E1 (100 A, 75 V).

SEM analysis of the nanomaterials obtained from the electrode shows the presence of flakes and large agglomerates, with particle sizes between 49 and 56 nm. The Raman spectra from the sample reveal a graphite structure, marked by the D bands at 1346 and 1356 cm^{-1} and the G band at 1580 cm^{-1} . The broad D-peak indicates that the sample has a low graphitization degree, with high disorder and numerous defects. The sample dis-

plays a heterogeneous nature. The graphitization degree is 53.7%, and the ID/IG ratio provides insight into the material's quality. The I2D/IG ratio (0.35 and 0.24) is much lower than the typical value for single-layer graphene (>1.6), while the IG/I2D ratio values of 2.87 and 4.13 suggest a low-layered nanomaterial. The ID/IG ratios of 0.97 and 0.59 imply a minimal presence of defects in the material (fig. 9,10).

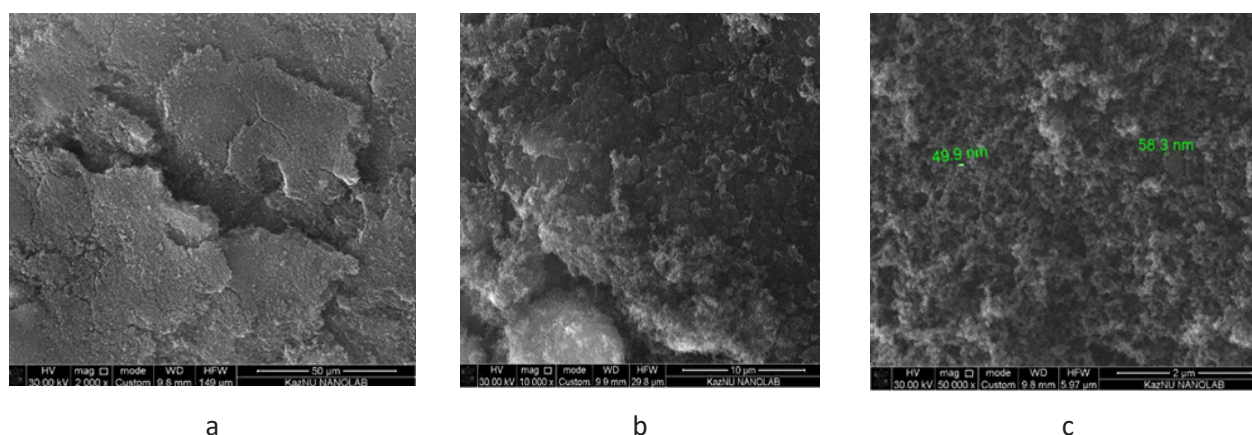
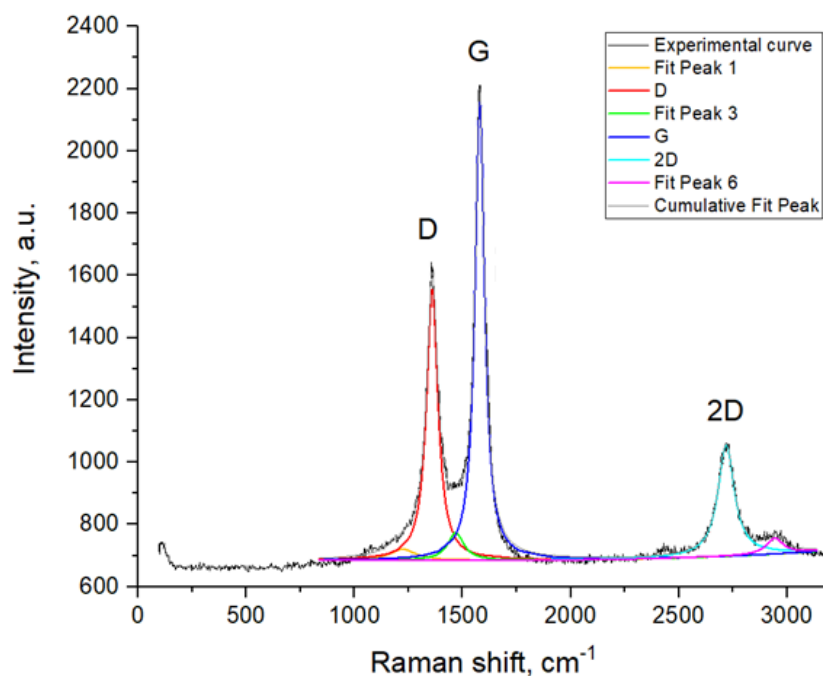


Figure 9 – SEM images of sample E2 (100 A, 75 V). a – x2000, b – x10000, c – x50000.



$$G_f = 53.7\%, I(D)/I(G) = 0.59, I(G)/I(D) = 1.69, I(G)/I(2D) = 4.13 \text{ (Lorentz)} \quad I(2D)/I(G) = 0.24$$

$$D = 1356 \text{ cm}^{-1}; G = 1580 \text{ cm}^{-1}; 2D = 2717 \text{ cm}^{-1}$$

Figure 10 – Raman spectrum of sample E2 (100 A, 75 V).

Among the four samples studied, sample E1 (electrode-derived material, gas-phase deposition) demonstrated the highest degree of graphitization (88.98%) and the lowest defect density, as indicated by its low ID/IG ratio and prominent 2D peak in the Raman spectrum. This superior structural order can be attributed to the localized high-temperature plasma environment near the electrode, which promotes more complete carbon rearrangement and crystallization into graphitic domains. In contrast, sample S1

(reactor wall deposit) exhibited a lower graphitization degree (36.08%) and higher defect density. This is likely due to the cooler, less controlled deposition environment along the reactor wall, which results in rapid quenching and disordered carbon structures. Samples S2 and E2 showed intermediate behavior, reflecting the influence of both deposition surface and gas-phase versus solid-state formation conditions.

These differences highlight the critical role of deposition location and temperature gradient in deter-

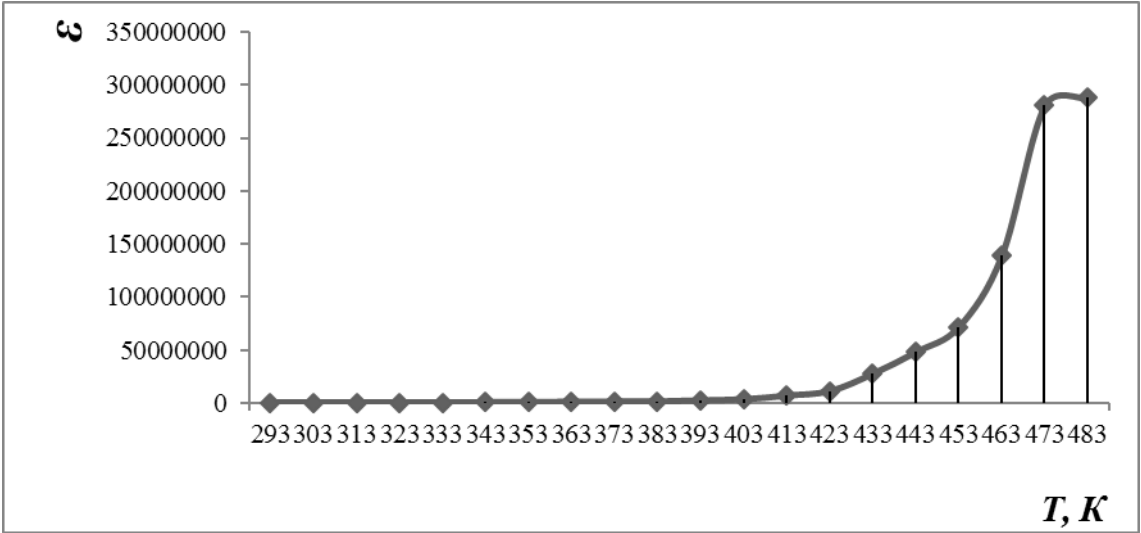
mining the structural quality of the resulting carbon nanomaterials. The electrode surface, being directly exposed to the arc core, provides the most favorable conditions for forming high-quality, low-defect CNTs and graphene-like layers.

The formation of flakes and spherical agglomerates observed in SEM images may result from two competing mechanisms: (1) layered growth from carbon atoms adsorbed on a substrate surface, and (2) volumetric nucleation in the gas phase, followed by aggregation during cooling. Overall, the nanostructure formation is primarily governed by carbon vapor concentration, local temperature, deposition rate, and surface properties of the collection zones – all of which

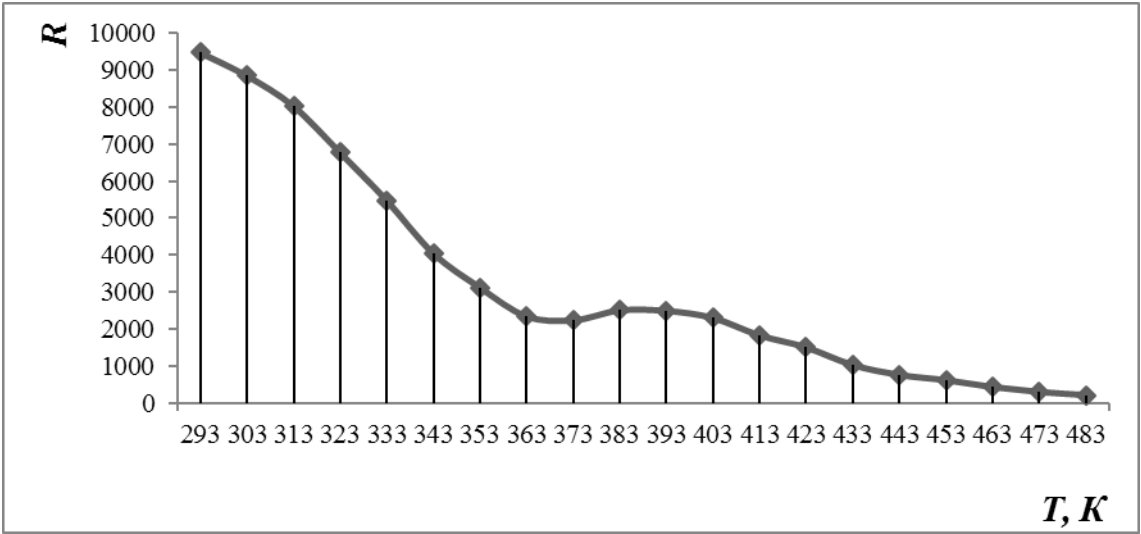
vary significantly across the different sample types.

The study focused on the electrophysical properties of carbon materials formed by the electric arc discharge method at 100 A, where a high graphitization degree was noted. Electrophysical measurements of carbon nanomaterials synthesized by the electric arc discharge method were carried out at a temperature of 293-483 K in the frequency ranges of 1, 5, and 10 kHz. Figure 11 shows how the dielectric constant (a) and electrical resistivity (b) of a carbon nanomaterial vary with temperature at frequencies of 1 kHz (I), 5 kHz (II), and 10 kHz (III).

Comparative data on the electrical properties of the resulting carbon materials are shown in Table 1.

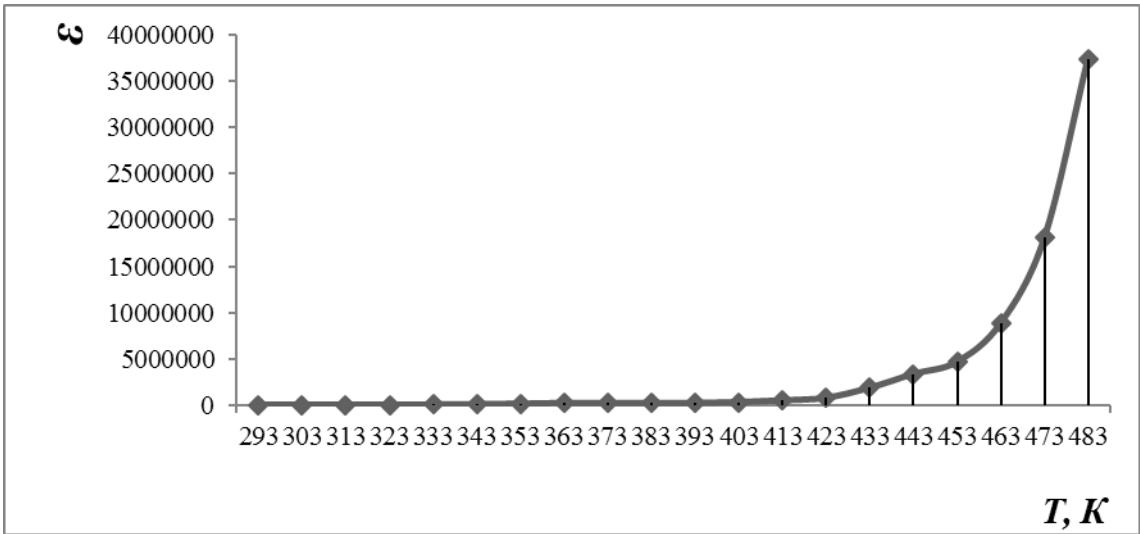


a)

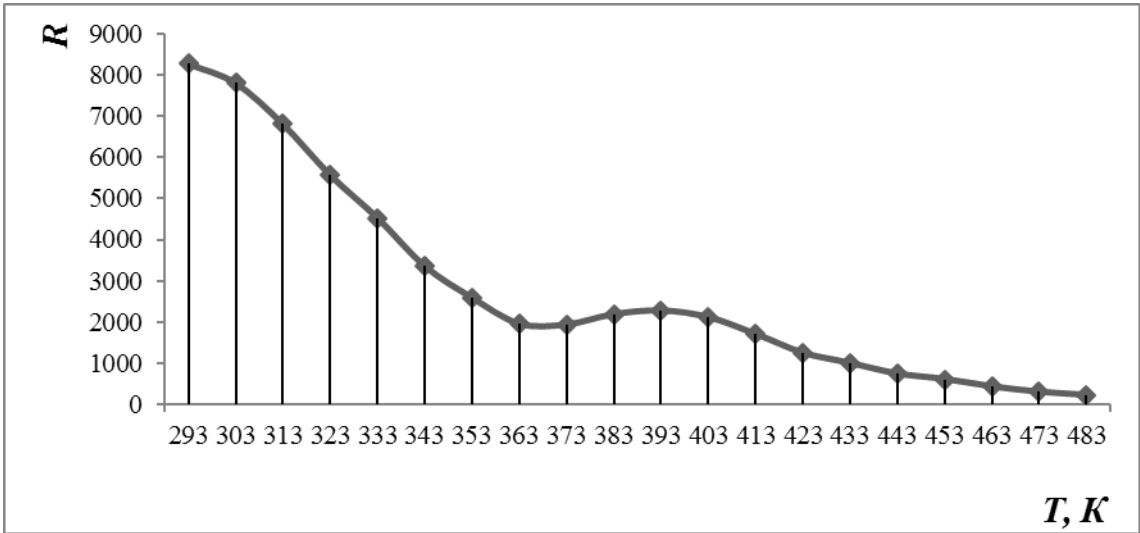


b)

I

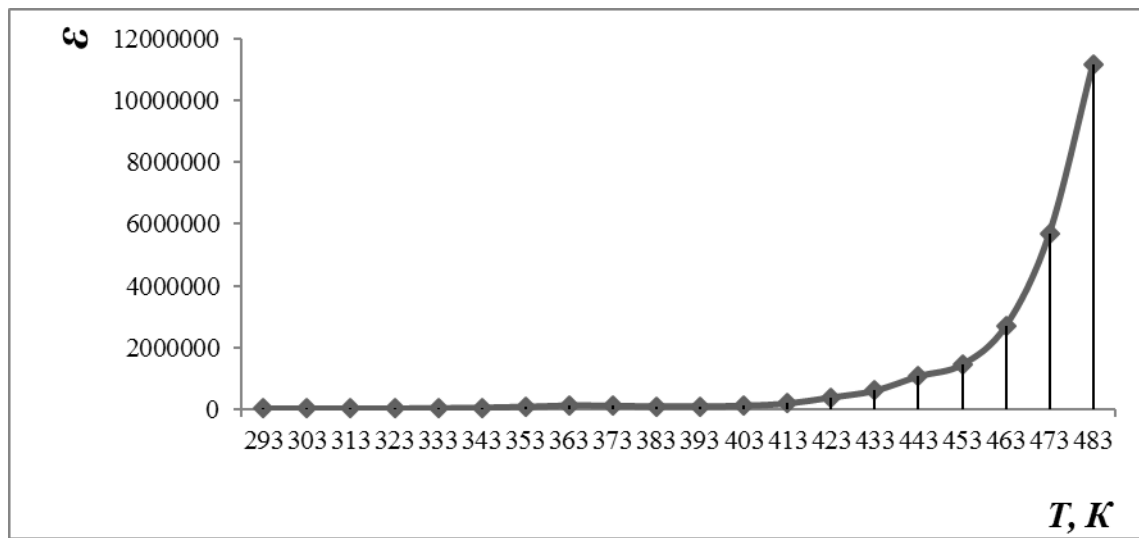


a)

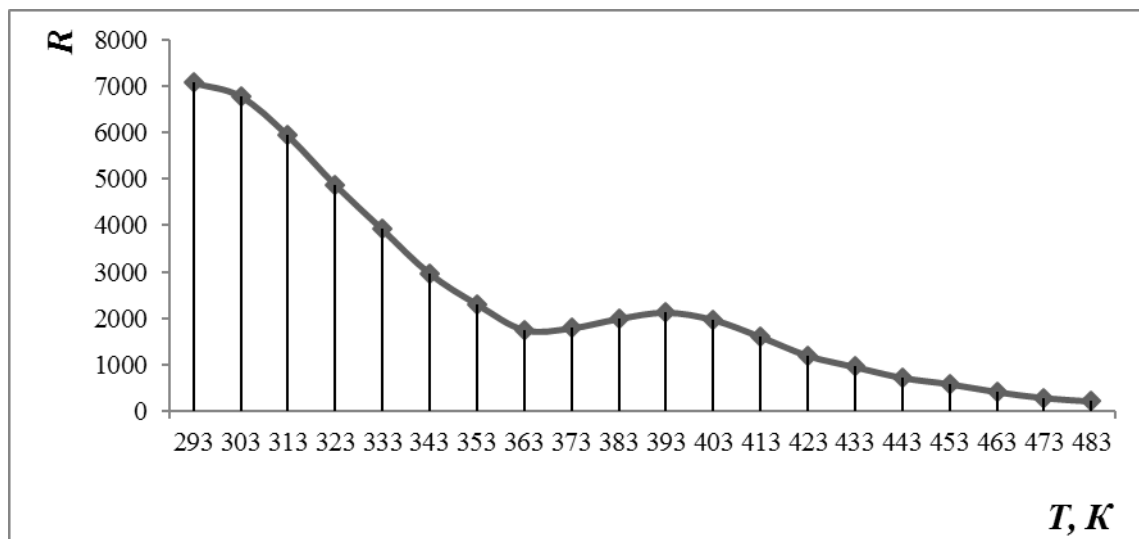


b)

II



a)



b)

III

Figure 11 – Variation of dielectric constant (a) and electrical resistivity (b) of carbon nanomaterial at different temperatures at frequencies of 1 kHz (I), 5 kHz (II) and 10 kHz (III).

Table 1 – Temperature dependence of electrical resistance (R), capacitance (C), and dielectric constant (ϵ)

Name of material	Dielectric constant (ϵ)					
	at 1 kHz		at 5 kHz		at 10 kHz	
	293 K	483 K	293 K	483 K	293 K	483 K
BaTiO ₃	1296	2159	1220	2102	561	2100
Nanomaterial	525877	287880816<	51819	37393213	24336	11181691
	Electrical resistance (lgR)					
	at 1 kHz		at 5 kHz		at 10 kHz	
	293 K	483 K	293 K	483 K	293 K	483 K
BaTiO ₃	4.13	3.67	4.47	3.58	5.18	3.37
Nanomaterial	3.98	2.35	3.92	2.35	3.85	2.34

The findings from investigations into the temperature dependence of the dielectric constant (ϵ) of a nanomaterial obtained at 100 A, 75 V show high ϵ values at all frequencies and in the range of 293-483 K. Thus, the ϵ values of this material at 293 K exceed ϵ of the reference BaTiO₃ by 406 times at 1 kHz, 42 times at 5 kHz and 43 times at 10 kHz. This mate-

rial holds promise for microcapacitor technology. The temperature dependence of its electrical resistance (R) reveals semiconductor conductivity from 293-363 K, metallic conductivity between 363-393 K, and again semiconductor conductivity from 393-483 K (at 10 kHz). According to the research, the band gap of this material is 0.72 eV within the 293-363 K range:

$$\Delta E = \frac{2 \times 0,000086173 \times 293 \times 363}{0,43(363 - 293)} \lg \frac{3,85}{3,24} = 0,72 \text{ eV} \quad (3)$$

In the temperature range of 493-483 K, the band gap of the material is 1.2 eV, which

classifies it as a narrow-bandgap semiconductor.

$$\Delta E = \frac{2 \times 0,000086173 \times 393 \times 483}{0,43(483 - 393)} \lg \frac{3,33}{2,34} = 1,2 \text{ eV} \quad (4)$$

It is important to highlight that the dielectric constant of the carbon materials produced is competitive with that of the new La_{15/8}Sr_{1/8}NiO₄, which has a remarkably high dielectric constant in the range of 10⁵-10⁶.

During the experiment, carbon materials containing graphene were synthesized using the electric arc discharge method, which is considered one of the most promising methods for producing nanomaterials, allowing for the production of products of relatively high purity and with few defects.

The nanomaterials synthesized, particularly sample E1, exhibited extremely high dielectric constants (ϵ), reaching up to 2.88×10^8 at 1 kHz and 483 K, significantly exceeding those of conventional dielectrics such as barium titanate (BaTiO₃), which typically ranges from 10³ to 10⁴ under similar conditions.

Compared to other carbon-based nanomaterials such as reduced graphene oxide or CNT-polymer composites, which generally exhibit ϵ values in the range of 10²-10⁴, the results obtained in this study suggest a remarkably high capacity for charge storage. Additionally, the observed semiconductor-to-metal transition with temperature and narrow band gap (0.72-1.2 eV) are comparable to or better than many reported CNT-based and graphene-based systems. These features suggest strong potential for application in microcapacitor technologies, temperature-sensitive electronic switches, and semiconducting layers in nanoelectronic devices, especially where high dielectric response and thermal stability are required.

The temperature range of 293-483 K selected for measuring the electrophysical properties refers to the post-synthesis characterization phase, not the

synthesis plasma itself. However, water cooling was implemented to control the local temperature of the sample collection surfaces (e.g., electrode and substrate) during and immediately after discharge, minimizing thermal damage and improving measurement repeatability.

Regarding plasma temperature control, water cooling does not significantly reduce the central arc plasma temperature (typically several thousand K), but it plays a crucial role in moderating the surrounding reactor wall and electrode temperatures, which directly affect deposition morphology, particle agglomeration, and cooling rates of the carbon nanomaterials. This indirectly influences crystallinity and defect formation.

A direct comparative analysis of synthesis outcomes with and without cooling was not the primary focus of this study, but will be considered in future work.

4 Conclusion

In this study, carbon nanomaterials were successfully synthesized using an electric arc discharge method with a copper substrate and characterized through SEM, Raman spectroscopy, and electrical measurements. A key novelty lies in the use of a copper substrate and controlled collection zones (electrode, substrate, wall), which revealed strong spatial

effects on graphitization quality, defect density, and morphology. Among the four samples, the electrode-derived nanomaterial (E1) showed the highest graphitization degree (88.98%) and the lowest defect content, highlighting the importance of deposition environment and thermal gradients in tailoring nanomaterial properties.

Importantly, the synthesized materials exhibited ultra-high dielectric constants and a tunable semi-conducting-to-metallic transition, positioning them as promising candidates for next-generation micro-capacitors, sensors, and thermally responsive nanoelectronic devices.

Future work should explore scaling the process for industrial production, optimizing substrate materials, and integrating these nanomaterials into functional electronic or energy storage systems. Additionally, a deeper investigation into long-term stability, conductivity under varying environments, and mechanical properties will be valuable for broadening application potential.

Acknowledgements. This research has been funded by the Science Committee of the Ministry of Science and Higher Education of the Republic of Kazakhstan (Grant No. AP19577512 “Development of scientific and technical bases for obtaining microporous carbon nanomaterials for hydrogen separation and storage”).

References

1. Il'in, A. M., Messerle, V. E., & Ustimenko, A. B. The formation of carbon nanotubes on copper electrodes under the arc discharge conditions // *High Energy Chemistry*. – 2010. – Vol. 44. – P. 326-331. <https://doi.org/10.1134/S0018143910040120>
2. Lozano-Castelló, D., Suárez-García, F., Alcañiz-Monge, J., Cazorla-Amorós, D., Linares-Solano, A. Gas-Adsorbing Nanoporous Carbons. – CRC Press: In *Carbon Nanomaterials Sourcebook*. – 2018. – P. 465-486.
3. Bardhan, N. M. 30 years of advances in functionalization of carbon nanomaterials for biomedical applications: a practical review // *Journal of Materials Research*. – 2017. – Vol. 32. –Is. 1. – P. 107-127. <https://doi.org/10.1557/jmr.2016.449>
4. Khamdohov, E. Z., Teshev, R. S., Khamdohov, Z. M., Khamdohov, A. Z., Kalajokov, Z. H., Kalajokov, H. H. Production of carbon films by the electric arc sputtering of graphite in a magnetic field // *Journal of Surface Investigation. X-ray, Synchrotron and Neutron Techniques*. – 2014. – Vol. 8. – P. 1306-1310. <https://doi.org/10.1134/S1027451014060317>
5. Wang, X., Li, Q., Xie, J., Jin, Z., Wang, J., Li, Y., Fan, S. Fabrication of ultralong and electrically uniform single-walled carbon nanotubes on clean substrates // *Nano letters*. – 2009. – Vol. 9. –Is. 9. – P. 3137-3141. <https://doi.org/10.1021/nl901260b>
6. Mittal, G., Dhand, V., Rhee, K. Y., Park, S. J., Lee, W. R. A review on carbon nanotubes and graphene as fillers in reinforced polymer nanocomposites // *Journal of industrial and engineering chemistry*. – 2015. – Vol. 21. – P. 11-25. <https://doi.org/10.1016/j.jiec.2014.03.022>
7. Abbas, A., Al-Amer, A. M., Laoui, T., Al-Marri, M. J., Nasser, M. S., Khraisheh, M., Atieh, M. A. Heavy metal removal from aqueous solution by advanced carbon nanotubes: critical review of adsorption applications // *Separation and Purification Technology*. – 2016. – Vol. 157. – P. 141-161. <https://doi.org/10.1016/j.seppur.2015.11.039>
8. Das, R., Ali, M. E., Abd Hamid, S. B., Ramakrishna, S., Chowdhury, Z. Z. Carbon nanotube membranes for water purification: A bright future in water desalination // *Desalination*. – 2014. – Vol. 336. – P. 97-109. <https://doi.org/10.1016/j.desal.2013.12.026>
9. Liu, X., Wang, M., Zhang, S., Pan, B. Application potential of carbon nanotubes in water treatment: a review // *Journal of Environmental Sciences*. – 2013. – Vol. 25. –Is. 7. – P. 1263-1280. [https://doi.org/10.1016/S1001-0742\(12\)60161-2](https://doi.org/10.1016/S1001-0742(12)60161-2)

10. Ng K. W., Lam W. H., Pichiah S. A review on potential applications of carbon nanotubes in marine current turbines // *Renewable and Sustainable Energy Reviews*. – 2013. – Vol. 28. – P. 331-339. <https://doi.org/10.1016/j.rser.2013.08.018>
11. Liu, W. W., Chai, S. P., Mohamed, A. R., & Hashim, U. Synthesis and characterization of graphene and carbon nanotubes: A review on the past and recent developments // *Journal of Industrial and Engineering Chemistry*. – 2014. – Vol. 20. – Is. 4. – P. 1171-1185. <https://doi.org/10.1016/j.jiec.2013.08.028>
12. Ying, L. S., bin Mohd Salleh, M. A., Rashid, S. B. A. Continuous production of carbon nanotubes—A review // *Journal of Industrial and Engineering Chemistry*. – 2011. – Vol. 17. – Is. 3. – P. 367-376. <https://doi.org/10.1016/j.jiec.2011.05.007>
13. Marsh H., Reinoso F. R. Activated carbon. Amsterdam: Elsevier. – 2006.
14. Dresselhaus, M. S., Dresselhaus, G., Eklund, P. C., Saito, R. Electrons and phonons in fullerenes. Optical and Electronic Properties of Fullerenes and Fullerene-Based Materials. – 1999. – P. 217.
15. Tian, Y., Zhang, Y., Wang, B., Ji, W., Zhang, Y., Xie, K. Coal-derived carbon nanotubes by thermal plasma jet // *Carbon*. – 2004. – Vol. 42. – Is. 12-13. – P. 2597-2601. <https://doi.org/10.1016/j.apmt.2018.06.007>
16. Yermagambet, B. T., Kazankapova, M. K., Borisenko, A. V., Nurgaliyev, N. U., Kasenova, Zh. M., Sayranbek, A., Kanagatov, K. G., Nauryzbaeva, A. T. Synthesis of carbon nanotubes by the method of CVD on the surface of the hydrophobic zone of the oil shale // *News of the Academy of Sciences of the Republic of Kazakhstan . Series of Geology and Technical Sciences*. – 2019. – Vol. 5. – Is. – 437. – P. 177-188. <https://doi.org/10.32014/2019.2518-170X.140>
17. Mohammad, M. I., Moosa, A. A., Potgieter, J. H., Ismael, M. K. Carbon nanotubes synthesis via arc discharge with a yttria catalyst // *International Scholarly Research Notices*. – 2013. – Vol. 1. – P. 785160. <https://doi.org/10.1155/2013/785160>
18. Rud, A. D., Kuskova, N. I., Ivaschuk, L. I., Boguslavskii, L. Z., Perekos, A. E. Synthesis of carbon nanomaterials using high-voltage electric discharge techniques by MM Rahman. InTech.–Rijeka. – 2011. – P. 99-116.
19. Perez-Cabero, M., Rodriguez-Ramos, I., & Guerrero-Ruiz, A. Characterization of carbon nanotubes and carbon nanofibers prepared by catalytic decomposition of acetylene in a fluidized bed reactor // *Journal of catalysis*. – 2003. – Vol. 215. – Is. 2. – P. 305-316. [https://doi.org/10.1016/S0021-9517\(03\)00026-5](https://doi.org/10.1016/S0021-9517(03)00026-5)
20. Yang, Z., Zhang, Q., Luo, G., Huang, J. Q., Zhao, M. Q., Wei, F. Coupled process of plastics pyrolysis and chemical vapor deposition for controllable synthesis of vertically aligned carbon nanotube arrays // *Applied Physics A*. – 2010. – Vol. 100. – P. 533-540. <https://doi.org/10.1007/s00339-010-5868-9>
21. Roslan, M. S., Abd Rahman, M. M., Jofri, M. H., Chaudary, K. T., Mohamad, A., Ali, J. Fullerene-to-MWCNT structural evolution synthesized by arc discharge plasma // *Journal of Carbon Research*. – 2018. – Vol. 4. – Is. 4. – P. 58. <https://doi.org/10.3390/c4040058>
22. Ranszewski, G. Optimization of the carbon nanotubes synthesis in arc discharge systems // *COMPEL-The international journal for computation and mathematics in electrical and electronic engineering*. – 2018. – Vol. 37. – Is. 5. – P. 1618-1625. <https://doi.org/10.1108/COMPEL-01-2018-0019>
23. Zhang, D., Ye, K., Yao, Y., Liang, F., Qu, T., Ma, W., Watanabe, T. Controllable synthesis of carbon nanomaterials by direct current arc discharge from the inner wall of the chamber // *Carbon*. – 2019. – Vol. 142. – P. 278-284. <https://doi.org/10.1016/j.carbon.2018.10.062>
24. Zaikovskii, A., Novopashin, S., Maltsev, V., Kardash, T., Shundrina, I. Tin-carbon nanomaterial formation in a helium atmosphere during arc-discharge // *RSC advances*. – 2019. – Vol. 9. – Is. 63. – P. 36621-36630. <https://doi.org/10.1039/C9RA05485E>
25. Ma, X., Li, S., Chaudhary, R., Hessel, V., Gallucci, F. Carbon nanosheets synthesis in a gliding arc reactor: on the reaction routes and process parameters // *Plasma Chemistry and Plasma Processing*. – 2021. – Vol. 41. – P. 191-209. <https://doi.org/10.1007/s11090-020-10120-z>
26. Yatom, S., Khrabry, A., Mitrani, J., Khodak, A., Kaganovich, I., Vekselman, V., Raitses, Y. Synthesis of nanoparticles in carbon arc: measurements and modeling // *MRS communications*. – 2018. – Vol. 8. – Is. 3. – P. 842-849. <https://doi.org/10.1557/mrc.2018.91>
27. Yermagambet, B. T., Kazankapova, M. K., Kasenov, B. K., Aitmagambetova, A. Z., Kuanyshbekov, E. E. Synthesis of graphene-containing nanomaterials based on a carbon product using electric arc discharge // *Solid Fuel Chemistry*. – 2021. – Vol. 55. – P. 380-390. <https://doi.org/10.3103/S0361521921060057>
28. Komokhov, P. G., Svatovskaya, L. B., Solovyova, V. Y., Sychev, A. M. High-strength concrete based on elements of nanotechnology using the sol-gel method, Achievements, problems and perspective directions of development of theory and practice of building materials science, Tenth Academic Readings of the RAASN. – 2006.

Information about authors:

Kazankapova Maira, PhD, Associate Professor, Corresponding Member of KazNANS, Leading Researcher, Head of Laboratory of LLP “Institute of Coal Chemistry and Technology” (Astana, Kazakhstan), e-mail: maira_1986@mail.ru

Yermagambet Bolat, Doctor of Chemical Sciences, Professor, Academician of KazNANS, Project Manager, Chief Researcher, Director of LLP “Institute of Coal Chemistry and Technology” (Astana, Kazakhstan), e-mail: bake.yer@mail.ru

Kasenov Bulat, Doctor of Chemical Sciences, Professor. Head Laboratory of the Chemical-Metallurgical Institute named after Zh.Abisheva (Karaganda, Kazakhstan), e-mail: kasenov1946@mail.ru

Kassenova Zhanar, Candidate of Chemical Sciences (PhD), Member of KazNANS, Leading Researcher is a Deputy Director of LLP "Institute of Coal Chemistry and Technology" (Astana, Kazakhstan), e-mail: zhanar_k_68@mail.ru

Malgazhdarova Ainagul is a Junior Researcher at the «Institute of Coal Chemistry and Technology», master student at the Eurasian National University of L.N. Gumilyov (Astana, Kazakhstan), e-mail: malgazhdarova.ab@mail.ru

Mendaliyev Gani is a Junior Researcher at the «Institute of Coal Chemistry and Technology», master student at the Eurasian National University of L.N. Gumilyov (Astana, Kazakhstan), e-mail: ganimen02@mail.ru

Akshekina Assel is a Senior Lab Assistant at the «Institute of Coal Chemistry and Technology», master student at the Eurasian National University of L.N. Gumilyov (Astana, Kazakhstan), e-mail: akshekina11@gmail.com

Kozhamuratova Ultugan is a Junior Researcher at the «Institute of Coal Chemistry and Technology», master student at the Eurasian National University of L.N. Gumilyov (Astana, Kazakhstan), e-mail: kozhamuratova.u@mail.ru